

High Fidelity 12-Mode Quantum Photonic Processor Operating at InGaAs Quantum Dot Wavelength

Michiel de Goede,* Henk Snijders, Pim Venderbosch, Ben Kassenberg,
Narasimhan Kannan, Devin H. Smith, Caterina Taballione,
Jörn P. Epping, Hans van den Vlekkert, and Jelmer J. Renema
QuiX Quantum B.V., 7521 AN Enschede, The Netherlands

(Dated: April 13, 2022)

arXiv:2204.05768v1 [quant-ph] 12 Apr 2022

Abstract

Reconfigurable quantum photonic processors are an essential technology for photonic quantum computing. Although most large-scale reconfigurable quantum photonic processors were demonstrated at the telecommunications C band around 1550 nm, high-performance single photon light sources utilizing quantum dots that are well-suited for photonic quantum computing operate at a variety of wavelengths. Thus, a demand exists for the compatibility of quantum photonic processors with a larger wavelength range. Silicon nitride (SiN) has a high confinement and wide transparency window, enabling compact, low-loss quantum photonic processors at wavelengths outside the C band. Here, we report a SiN universal 12-mode quantum photonic processor with optimal operation at a wavelength of 940 nm, which is compatible with InGaAs quantum dot light sources that emit light in the 900 nm to 970 nm wavelength range. The processor can implement arbitrary unitary transformations on its 12 input modes with a fidelity of 98.6%, with a mean optical loss of 3.4 dB/mode.

I. INTRODUCTION

Photonics is one of the most promising approaches to quantum computing, as it is one of the only two platforms to have demonstrated a quantum advantage so far [1], the other being based on superconducting qubits [2]. Photonic quantum computing benefits from the use of quantum states that both have a low decoherence, due to their weak interaction with the environment, and preserve their coherence at room temperature. Linear optics is the backbone of photonic quantum computing due to its simple generation of photon entanglement via quantum interference on a normal beamsplitter. A quantum photonic processor, i.e., a linear optical interferometer, is therefore the central component of a photonic quantum computer. A photonic processor requires universal reconfigurability to implement arbitrary transformations on the input optical states, low losses to preserve the quantum information, and must be large in scale to obtain the necessary complexity of the quantum computation. Integrated photonics meets these conditions and offers a scalable, mature, and commercially available tool for large-scale, phase-stable, and universally reconfigurable linear optical interferometers [3].

* m.degoede@quixquantum.com

Photonic quantum computing requires the integration of a photonic processor with a single photon light source that has both a high brightness and high indistinguishability. Quantum dot (QD) single photon sources are a mature technology that produces highly indistinguishable photons at a large rate [4, 5]. Currently, single-photon sources based on QDs can be reproducibly realized with an average indistinguishability of 90% and brightness—or photon emission probability per pulse—of 13% for single photon emission [6]. Furthermore, QDs can be integrated on chip in micropillars [4] or photonic crystals [7]. State of the art QDs operate in the 900 nm to 970 nm wavelength range. High quality QDs operating at longer wavelengths are much harder to produce because the physical dimensions of the QDs increases and they are then much more subject to material stress and impurities [8]. QD sources have been used for a wide variety of quantum information processing experiments such as Boson Sampling [9, 10], cluster state generation [11, 12] and quantum networks [13]. Despite these excellent properties, no photonic processors have been demonstrated that are compatible with the wavelength range of InGaAs QDs.

Various quantum photonic processors were previously demonstrated that operate at wavelengths in the telecommunications C band (1530 nm to 1565 nm) based on silicon-on-insulator (SOI) [14] or silicon nitride (SiN) [15]. In fact, the largest universal processor, supporting 20 modes was recently demonstrated on the SiN material platform with low-losses and a high degree of reconfigurability [16]. However, there is a lack of large-scale, fully reconfigurable quantum photonic processors operating at wavelengths outside the C band. There are some examples of processors capable of photonic quantum information processing in the 750 nm to 850 nm wavelength range, but they were either not universally reconfigurable [17–21], or small-scale with up to 6 modes [22, 23]. For realizing large-scale, low-loss photonic processors at a wide range of operating wavelengths, SiN is the most promising material due to its high optical confinement and integration density [24] and wide transparency window ranging from 400 nm to 2350 nm [25], which is compatible with the emission wavelength of InGaAs QD single photon sources as well as most other candidate single-photon emitters [26].

In this paper, we report a SiN high-fidelity, low-loss and universal quantum photonic processor designed for operation at 940 nm. The demonstrated operating wavelength allows integration with InGaAs quantum dots for a scalable approach towards photonic quantum computing.

II. THE QUANTUM PHOTONIC PROCESSOR

The quantum photonic processor consists out of three parts: a photonic integrated circuit of stoichiometric SiN symmetric double-stripe waveguides with the TriPleX technology [25], control electronics and control software. The device is optically packaged with input and output fiber arrays and electronically connected by wire-bonds to a control PCB, as shown in Fig.1a. The photonic chip contains a mesh of interconnected waveguides with 12 input and 12 output modes, enabling the implementation of arbitrary 12×12 unitary matrix transformations on the input light states. The network consists of a repeating unit cell that contains a tunable Mach-Zehnder interferometer (MZI) to set the relative amplitudes and an external phase shifter to set the relative phase of the two waveguides, as shown in Fig.1b, together forming an arbitrarily tunable beam-splitter. Both tunable elements are realized with thermo-optic phase actuators, of which there are 132 distributed over 66 unit cells. The phases required for a specific matrix transformation are determined based on the method of [27]. The phase actuators implement phase shifts by resistive heating, locally elevating the waveguide temperature and thus inducing a change in refractive index. The control electronics and control software ensure a stable device temperature during operation and implement the corresponding phases for arbitrary 12×12 unitary matrices.

The design of the SiN photonic chip was performed for operation around a central wavelength of 940 nm to allow for compatibility with the InGaAs emission wavelength range. The geometry consists of two identical SiN stripes separated by a gap and embedded in a silica glass cladding, as shown in Fig.1c. The waveguide geometry was constrained to only support a single (TE) mode, which also has low bend losses, allowing for small bend radii. We found an optimal design with a stripe width of 1000 nm, stripe height of 65 nm and a vertical gap of 250 nm. This design has low bend losses down to a radius of 110 μm . Finally, we designed a horizontal taper for a fiber-to-chip coupling spot-size converter with an expected coupling loss of 0.4 dB, which is crucial for quantum photonic computing since photon loss should be minimal to reduce overhead.

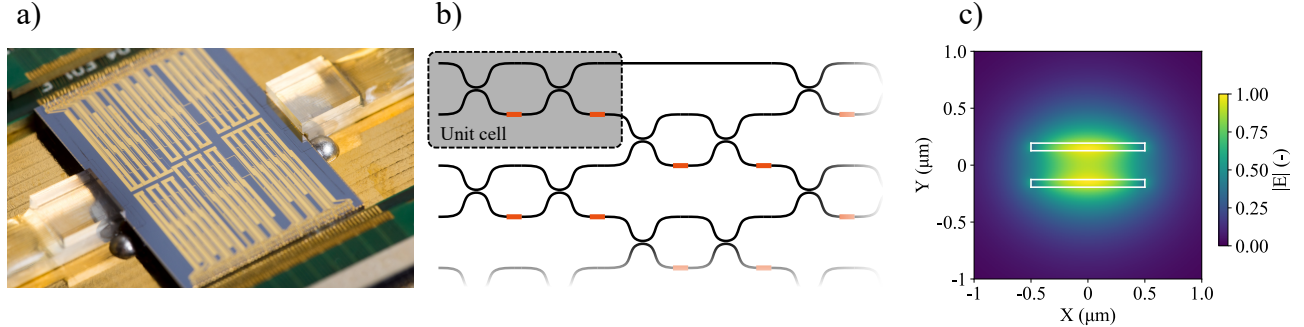


FIG. 1. **a)** Photograph of the 12-mode photonic processor chip ($16 \text{ mm} \times 22 \text{ mm}$). **b)** Functional design of the photonic network consisting of interconnected waveguide paths (black) and thermo-optic phase actuators (red). The network is built by repeating the unit cell, which contains a tunable beam splitter (TBS) and external phase shifter (PS). **c)** Simulated mode field profile of the supported TE mode for 940 nm of the optimal waveguide design. The simulation was performed by a fully vectorial 2D eigenmode calculation using Lumerical MODE solutions. The white lines indicate the symmetric double-stripe SiN waveguide within the silica glass cladding.

III. EXPERIMENTAL RESULTS

The quantum photonic processor was characterized by injecting coherent light at a wavelength of 940 nm into the device (TOPTICA FF Pro QD tunable laser). The light was guided into the photonic processor using a 1×12 PM fiber switch (Fibermart), followed by detection at an array of photodiodes (Thorlabs FGA01FC).

First, the phase-voltage relationship of the tunable thermo-optic phase actuators was characterized. Voltages were applied to each phase actuator while recording the output powers at the photodiodes, from which the phase response of each element was obtained. The average power for a 2π phase shift was 310 mW. Furthermore, we find that our directional couplers operate very close to the 3 dB power coupling point at the wavelength of 940 nm, as evidenced by an average tunable MZI extinction ratio of 22.4 dB. Next, the average insertion loss of the photonic processor was measured to be 3.4 dB, as shown in Fig. 2a. This includes the loss of the fiber-to-chip and chip-to-fiber coupling and propagation through the network with a path length of 10.7 cm. Finally, the reconfigurability of the photonic processor was characterized by generating, implementing, and measuring 100 Haar-random matrices on the network. The output intensity distribution was measured for each input mode of the

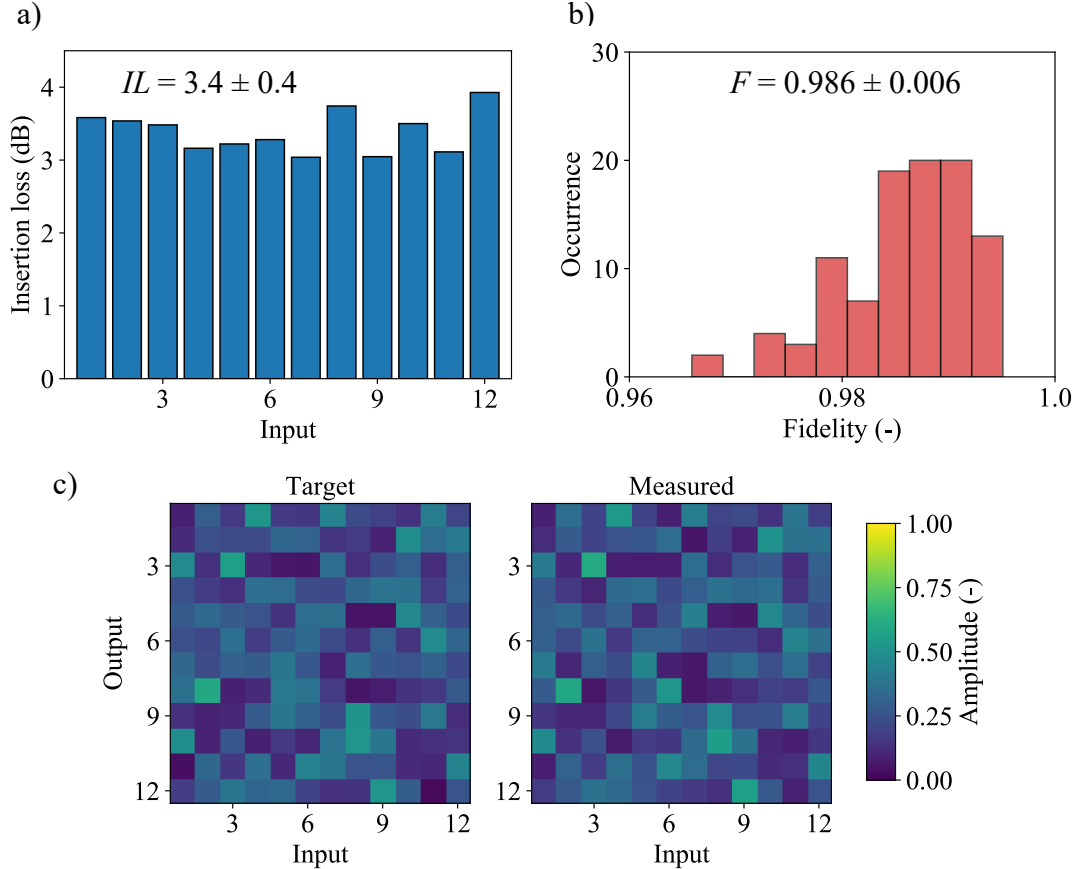


FIG. 2. Summary of the characterization. **a)** Measured insertion loss for each mode on the photonic chip. **b)** Distribution of the measured amplitude fidelities for 100 Haar-random matrices. **c)** Comparison between the amplitude distribution of an ideal Haar-random unitary matrix (target) with its experimental implementation (data).

matrices, followed by normalizing the data by correcting for the port-dependent coupling losses and photodiode dark counts. The fidelity measure of the matrices was then determined by $F = \text{Tr}(|U^+| \cdot |U_{\text{exp}}|) / 12$, where U is the target matrix and U_{exp} the measured, normalized matrix. We obtained an average fidelity of $F = 0.986 \pm 0.006$, as shown in Fig. 2b. As an example, Fig. 2c shows a comparison between one of the target Haar-random matrices (left), and the measured results from the implementation of that matrix on the processor with a fidelity of $F = 0.987$ (right).

IV. DISCUSSION AND CONCLUSIONS

Our work demonstrates the first large-scale, universally reconfigurable quantum photonic processor that operates at a wavelength range outside of the prevalent telecom C-band. The device has low insertion loss and a high degree of reconfigurability. Despite its smaller size and the reduced optical path length per mode, the insertion losses are higher than the previously demonstrated value of 2.9 dB/mode for a SiN 20-mode quantum photonic processor [16]. The higher loss results from the increased Rayleigh scattering at the lower wavelength range than that of the C band, which can be mitigated by improving the fabrication process. Furthermore, this device has more efficient heaters that require a lower power for a 2π phase shift than the other demonstrated large-scale SiN quantum photonic processors [15, 16]. This is beneficial for a lower thermal load, allowing a higher density of heaters integrated on the photonic circuit, and for a more precise reconfigurability and a higher fidelity. In fact, this improved the matrix fidelity compared with the 12-mode quantum photonic processor of [15].

The used material platform SiN benefits from a wide transparency window enabling operation at a wide range of wavelengths. The demonstrated operating wavelength of 940 nm is of specific interest for InGaAs-based quantum dot single photon sources that benefit from scalable fabrication and integration techniques. Furthermore, SiN is a highly versatile platform enabling fast switching [28], lowest propagation losses [29] and superconducting single-photon detectors [30, 31], thus presenting itself as a viable path towards fully integrated quantum computers.

-
- [1] H.-S. Zhong, H. Wang, Y.-H. Deng, M.-C. Chen, L.-C. Peng, Y.-H. Luo, J. Qin, D. Wu, X. Ding, Y. Hu, P. Hu, X.-Y. Yang, W.-J. Zhang, H. Li, Y. Li, X. Jiang, L. Gan, G. Yang, L. You, Z. Wang, L. Li, N.-L. Liu, C.-Y. Lu, and J.-W. Pan, Quantum computational advantage using photons, *Science* **370**, 1460 (2020), eprint: <https://www.science.org/doi/pdf/10.1126/science.abe8770>.
- [2] F. Arute, K. Arya, R. Babbush, D. Bacon, J. C. Bardin, R. Barends, R. Biswas, S. Boixo, F. G. S. L. Brandao, D. A. Buell, B. Burkett, Y. Chen, Z. Chen, B. Chiaro, R. Collins, W. Courtney, A. Dunsworth, E. Farhi, B. Foxen, A. Fowler, C. Gidney, M. Giustina, R. Graff, K. Guerin,

- S. Habegger, M. P. Harrigan, M. J. Hartmann, A. Ho, M. Hoffmann, T. Huang, T. S. Humble, S. V. Isakov, E. Jeffrey, Z. Jiang, D. Kafri, K. Kechedzhi, J. Kelly, P. V. Klimov, S. Knysh, A. Korotkov, F. Kostritsa, D. Landhuis, M. Lindmark, E. Lucero, D. Lyakh, S. Mandrà, J. R. McClean, M. McEwen, A. Megrant, X. Mi, K. Michielsen, M. Mohseni, J. Mutus, O. Naaman, M. Neeley, C. Neill, M. Y. Niu, E. Ostby, A. Petukhov, J. C. Platt, C. Quintana, E. G. Rieffel, P. Roushan, N. C. Rubin, D. Sank, K. J. Satzinger, V. Smelyanskiy, K. J. Sung, M. D. Trevithick, A. Vainsencher, B. Villalonga, T. White, Z. J. Yao, P. Yeh, A. Zalcman, H. Neven, and J. M. Martinis, Quantum supremacy using a programmable superconducting processor, *Nature* **574**, 505 (2019).
- [3] J. Wang, F. Sciarrino, A. Laing, and M. G. Thompson, Integrated photonic quantum technologies, *Nature Photonics* **14**, 273 (2020).
- [4] N. Somaschi, V. Giesz, L. De Santis, J. C. Loredo, M. P. Almeida, G. Hornecker, S. L. Portalupi, T. Grange, C. Antón, J. Demory, C. Gómez, I. Sagnes, N. D. Lanzillotti-Kimura, A. Lemaître, A. Auffeves, A. G. White, L. Lanco, and P. Senellart, Near-optimal single-photon sources in the solid state, *Nature Photonics* **10**, 340 (2016).
- [5] X. Ding, Y. He, Z.-C. Duan, N. Gregersen, M.-C. Chen, S. Unsleber, S. Maier, C. Schneider, M. Kamp, S. Höfling, C.-Y. Lu, and J.-W. Pan, On-demand single photons with high extraction efficiency and near-unity indistinguishability from a resonantly driven quantum dot in a micropillar, *Phys. Rev. Lett.* **116**, 020401 (2016).
- [6] H. Ollivier, I. Maillette de Buy Wenniger, S. Thomas, S. C. Wein, A. Harouri, G. Coppola, P. Hilaire, C. Millet, A. Lemaître, I. Sagnes, O. Krebs, L. Lanco, J. C. Loredo, C. Antón, N. Somaschi, and P. Senellart, Reproducibility of high-performance quantum dot single-photon sources, *ACS Photonics* **7**, 1050 (2020).
- [7] R. Uppu, F. T. Pedersen, Y. Wang, C. T. Olesen, C. Papon, X. Zhou, L. Midolo, S. Scholz, A. D. Wieck, A. Ludwig, and P. Lodahl, Scalable integrated single-photon source, *Science Advances* **6**, eabc8268 (2020), <https://www.science.org/doi/pdf/10.1126/sciadv.abc8268>.
- [8] P. Senellart, G. Solomon, and A. White, High-performance semiconductor quantum-dot single-photon sources, *Nature Nanotechnology* **12**, 1026 (2017).
- [9] J. C. Loredo, M. A. Broome, P. Hilaire, O. Gazzano, I. Sagnes, A. Lemaitre, M. P. Almeida, P. Senellart, and A. G. White, Boson sampling with single-photon fock states from a bright solid-state source, *Phys. Rev. Lett.* **118**, 130503 (2017).

- [10] H. Wang, Y. He, Y.-H. Li, Z.-E. Su, B. Li, H.-L. Huang, X. Ding, M.-C. Chen, C. Liu, J. Qin, J.-P. Li, Y.-M. He, C. Schneider, M. Kamp, C.-Z. Peng, S. Höfling, C.-Y. Lu, and J.-W. Pan, High-efficiency multiphoton boson sampling, *Nature Photonics* **11**, 361 (2017).
- [11] D. Istrati, Y. Pilnyak, L. Cohen, H. S. Eisenberg, C. Anton-Solanas, J. C. L. Rosillo, P. Hilaire, H. Ollivier, C. Millet, A. Lemaître, I. Sagnes, A. Harouri, L. Lanco, and P. Senellart, Generating multi-photon entangled states from a single deterministic single-photon source, in *Quantum Information and Measurement (QIM) V: Quantum Technologies* (Optica Publishing Group, 2019) p. T3B.1.
- [12] I. Schwartz, D. Cogan, E. R. Schmidgall, Y. Don, L. Gantz, O. Kenneth, N. H. Lindner, and D. Gershoni, Deterministic generation of a cluster state of entangled photons, *Science* **354**, 434 (2016), <https://www.science.org/doi/pdf/10.1126/science.aah4758>.
- [13] C.-Y. Lu and J.-W. Pan, Quantum-dot single-photon sources for the quantum internet, *Nature Nanotechnology* **16**, 1294 (2021).
- [14] N. C. Harris, G. R. Steinbrecher, M. Prabhu, Y. Lahini, J. Mower, D. Bunandar, C. Chen, F. N. C. Wong, T. Baehr-Jones, M. Hochberg, S. Lloyd, and D. Englund, Quantum transport simulations in a programmable nanophotonic processor, *Nature Photonics* **11**, 447 (2017), number: 7.
- [15] C. Taballione, R. v. d. Meer, H. J. Snijders, P. Hooijschuur, J. P. Epping, M. d. Goede, B. Kassenberg, P. Venderbosch, C. Toebes, H. v. d. Vlekkert, P. W. H. Pinkse, and J. J. Renema, A universal fully reconfigurable 12-mode quantum photonic processor, *Materials for Quantum Technology* **1**, 035002 (2021), publisher: IOP Publishing.
- [16] C. Taballione, M. C. Anguita, M. de Goede, P. Venderbosch, B. Kassenberg, H. Snijders, N. Kannan, D. Smith, J. P. Epping, R. van der Meer, P. W. H. Pinkse, H. v. d. Vlekkert, and J. J. Renema, 20-mode universal quantum photonic processor (2022).
- [17] A. Crespi, R. Osellame, R. Ramponi, D. J. Brod, E. F. Galvão, N. Spagnolo, C. Vitelli, E. Maiorino, P. Mataloni, and F. Sciarrino, Integrated multimode interferometers with arbitrary designs for photonic boson sampling, *Nature Photonics* **7**, 545 (2013).
- [18] M. Dong, G. Clark, A. J. Leenheer, M. Zimmermann, D. Dominguez, A. J. Menssen, D. Heim, G. Gilbert, D. Englund, and M. Eichenfield, High-speed programmable photonic circuits in a cryogenically compatible, visible–near-infrared 200 mm cmos architecture, *Nature Photonics* **16**, 59 (2022).

- [19] F. Hoch, S. Piacentini, T. Giordani, Z.-N. Tian, M. Iuliano, C. Esposito, A. Camillini, G. Carvacho, F. Ceccarelli, N. Spagnolo, A. Crespi, F. Sciarrino, and R. Osellame, Boson sampling in a reconfigurable continuously-coupled 3d photonic circuit (2021).
- [20] M. Tillmann, B. Dakić, R. Heilmann, S. Nolte, A. Szameit, and P. Walther, Experimental boson sampling, *Nature Photonics* **7**, 540 (2013), number: 7.
- [21] J. B. Spring, B. J. Metcalf, P. C. Humphreys, W. S. Kolthammer, X.-M. Jin, M. Barbieri, A. Datta, N. Thomas-Peter, N. K. Langford, D. Kundys, J. C. Gates, B. J. Smith, P. G. R. Smith, and I. A. Walmsley, Boson Sampling on a Photonic Chip, *Science* **339**, 798 (2013), number: 6121.
- [22] J. Carolan, C. Harrold, C. Sparrow, E. Martín-López, N. J. Russell, J. W. Silverstone, P. J. Shadbolt, N. Matsuda, M. Oguma, M. Itoh, G. D. Marshall, M. G. Thompson, J. C. F. Matthews, T. Hashimoto, J. L. O'Brien, and A. Laing, Universal linear optics, *Science* **349**, 711 (2015), number: 6249.
- [23] P. L. Mennea, W. R. Clements, D. H. Smith, J. C. Gates, B. J. Metcalf, R. H. S. Bannerman, R. Burgwal, J. J. Renema, W. S. Kolthammer, I. A. Walmsley, and P. G. R. Smith, Modular linear optical circuits, *Optica* **5**, 1087 (2018), publisher: OSA.
- [24] C. Taballione, T. A. W. Wolterink, J. Lugani, A. Eckstein, B. A. Bell, R. Grootjans, I. Visscher, D. Geskus, C. G. H. Roeloffzen, J. J. Renema, I. A. Walmsley, P. W. H. Pinkse, and K.-J. Boller, 8×8 reconfigurable quantum photonic processor based on silicon nitride waveguides, *Optics Express* **27**, 26842 (2019), number: 19 Publisher: OSA.
- [25] C. G. H. Roeloffzen, M. Hoekman, E. J. Klein, L. S. Wevers, R. B. Timens, D. Marchenko, D. Geskus, R. Dekker, A. Alippi, R. Grootjans, A. van Rees, R. M. Oldenbeuving, J. P. Epping, R. G. Heideman, K. Wörhoff, A. Leinse, D. Geuzebroek, E. Schreuder, P. W. L. van Dijk, I. Visscher, C. Taddei, Y. Fan, C. Taballione, Y. Liu, D. Marpaung, L. Zhuang, M. Benelajla, and K. Boller, Low-Loss Si₃N₄ TriPleX Optical Waveguides: Technology and Applications Overview, *IEEE Journal of Selected Topics in Quantum Electronics* **24**, 1 (2018), number: 4.
- [26] M. D. Eisaman, J. Fan, A. Migdall, and S. V. Polyakov, Invited review article: Single-photon sources and detectors, *Review of scientific instruments* **82**, 071101 (2011).
- [27] W. R. Clements, P. C. Humphreys, B. J. Metcalf, W. S. Kolthammer, and I. A. Walmsley, Optimal design for universal multiport interferometers, *Optica* **3**, 1460 (2016), number: 12 Publisher: OSA.

- [28] J. P. Epping, D. Marchenko, A. Leinse, R. Mateman, M. Hoekman, L. Wevers, E. J. Klein, C. G. H. Roeloffzen, M. Dekkers, and R. Heilmann, Ultra-low-power stress-based phase actuator for microwave photonics, 2017 European Conference on Lasers and Electro-Optics and European Quantum Electronics Conference **CK_7_6** (2017), journal Abbreviation: CLEO_Europe.
- [29] J. F. Bauters, M. J. R. Heck, D. D. John, J. S. Barton, C. M. Bruinink, A. Leinse, R. G. Heideman, D. J. Blumenthal, and J. E. Bowers, Planar waveguides with less than 0.1 dB/m propagation loss fabricated with wafer bonding, *Opt. Express* **19**, 24090 (2011), publisher: OSA.
- [30] C. Schuck, W. H. P. Pernice, and H. X. Tang, NbTiN superconducting nanowire detectors for visible and telecom wavelengths single photon counting on Si₃N₄ photonic circuits, *Applied Physics Letters* **102**, 051101 (2013), number: 5 Publisher: American Institute of Physics.
- [31] C. Schuck, X. Guo, L. Fan, X. Ma, M. Poot, and H. X. Tang, Quantum interference in heterogeneous superconducting-photonic circuits on a silicon chip, *Nature Communications* **7**, 10352 (2016), number: 1.